Electronic supplementary information

Synthesis of vanadium oxide hydrate $H_2V_3O_8$ nanobelts

Vanadium pentoxide (V_2O_5), ethanol, and Glucose ($C_6H_{12}O_6 \cdot H_2O$) with analytical grade were purchased from Sinopharm Chemical Reagent Co., Ltd and used without any further purification. The synthesis of vanadium oxide hydrate $H_2V_3O_8$ nanobelts was based on our previous report [1]. In a typical synthesis, 1.82 g of V_2O_5 powder was dispersed into 5 mL of ethanol, and then 75 mL of deionized water was added into the above solution with magnetic stirring. The mixed solution was transferred into a 100 mL Teflon Lined stainless steel autoclave after the solution became suspension. The autoclave was sealed and maintained at 180 °C for 48 h and then cooled to room temperature naturally. The products were filtered off, washed with distilled water and absolute ethanol several times to remove any possible residue, and dried in vacuum at 75 °C for future application.

Synthesis of $H_2V_3O_8$@C core-shell composites

The synthesis of $H_2V_3O_8$@C core-shell composite was according to our previous reports [2, 3]. In a typical procedure, 0.5 g of the as-obtained $H_2V_3O_8$ nanobelts were dispersed into the glucose solution (3.0 g of glucose and 60 mL of distilled water) in a 100 mL beaker under ultrasonic for 20 min, and then the mixture was stirred vigorously for 1 h by magnetic stirrer. After the solution became suspension, they were transferred into a 100 mL Teflon Lined stainless steel autoclave, which was sealed and maintained at 180 °C for 4 h. After cooling to room temperature naturally, the products were filtered off, washed with distilled water and absolute ethanol several times, and dried in vacuum at 75 °C for further characterization and application.

Figure S1

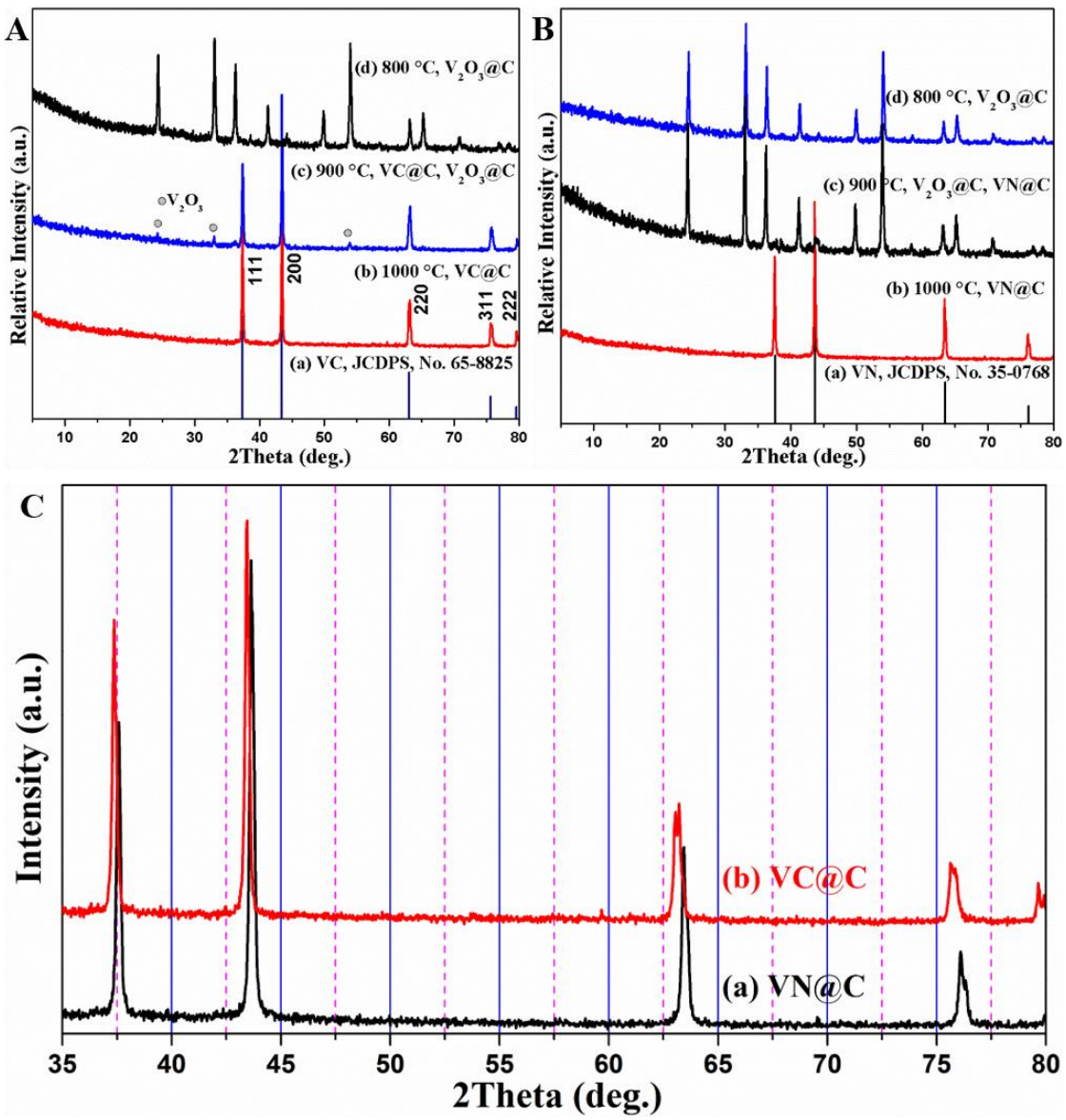

Figure S1. XRD patterns of the samples obtained at various calcined temperatures for 2 h: (A) VC@C series; (B) VN@C series; (C) Identification of the differences of VC@C and VN@C.

Figure S2

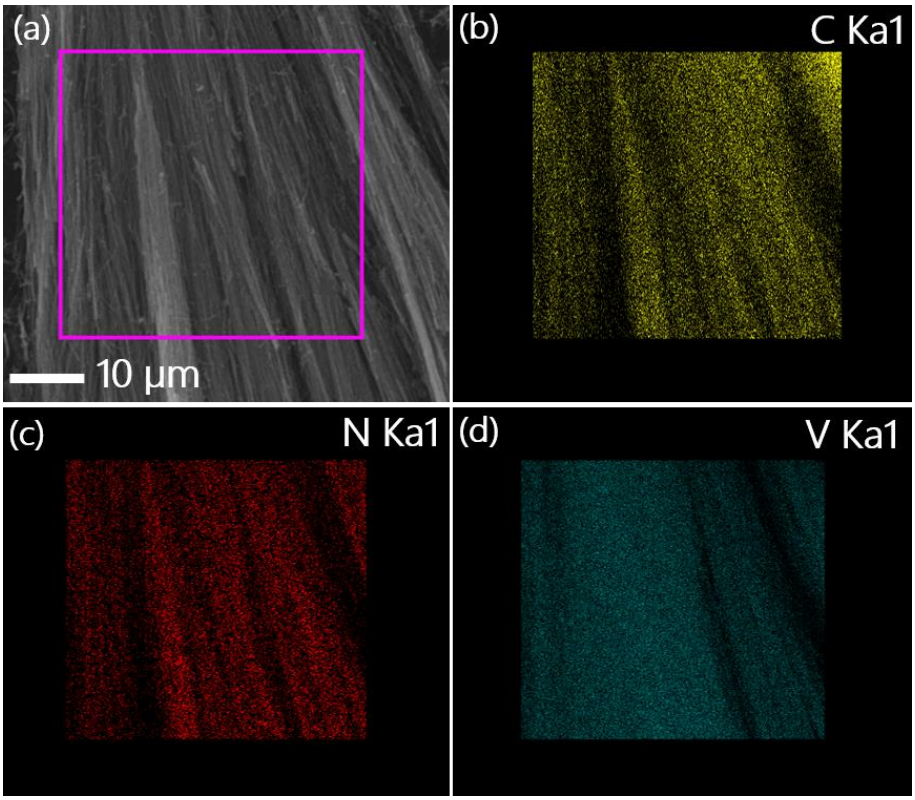

Figure S2. SEM image of VN@C and the corresponding elemental mapping images.

Figure S3

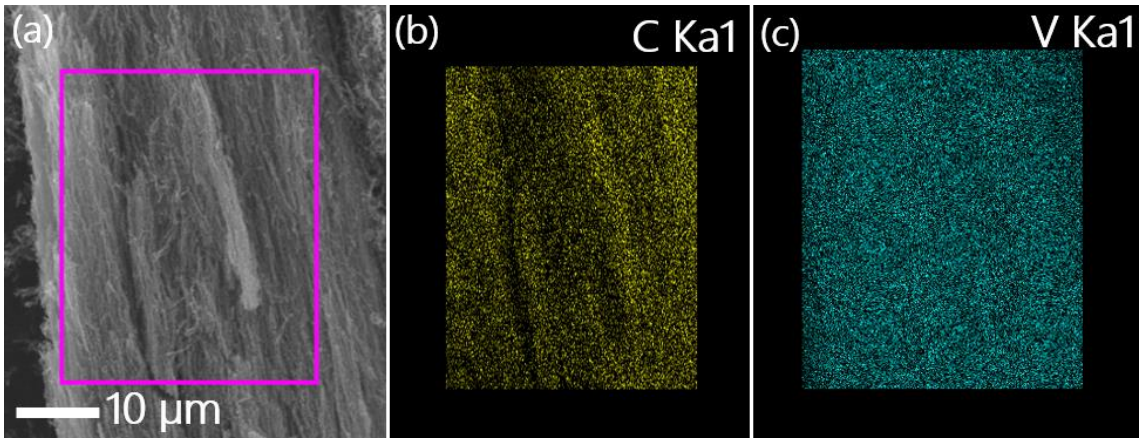

Figure S3. SEM image of VC@C and the corresponding elemental mapping images.

Figure S4

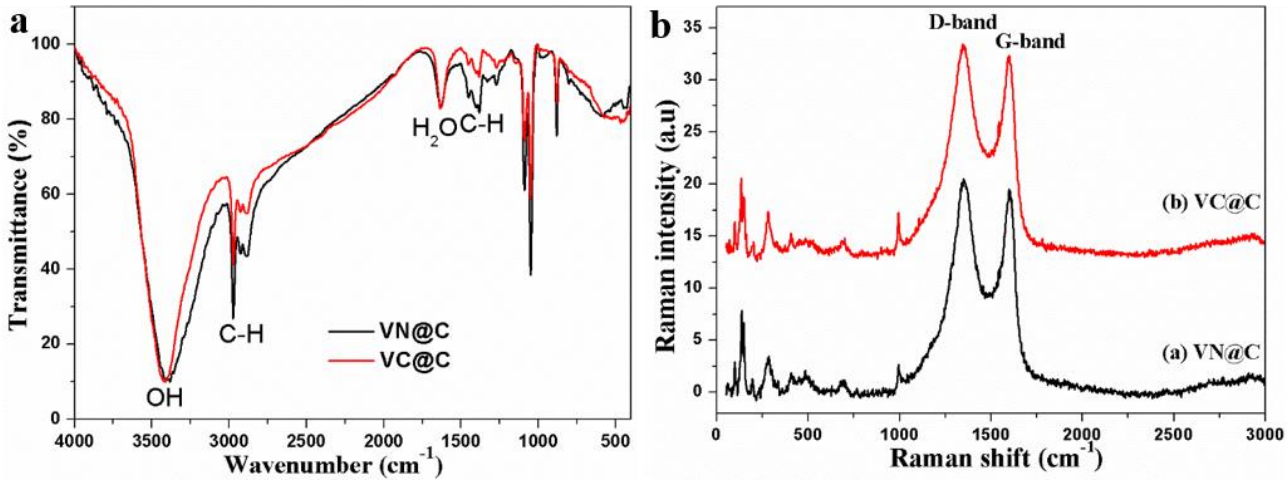

Figure S4. FTIR (a) and Raman (b) spectra of VN@C and VC@C.

Figure S5

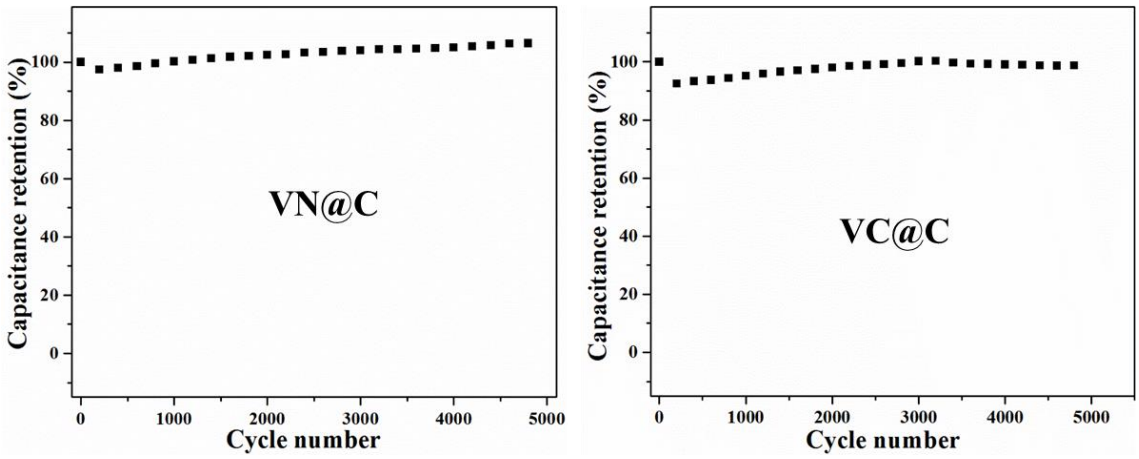

Figure S5. The cycling stability of the as-fabricated VC@C and VN@C SSC electrodes.

Figure S6

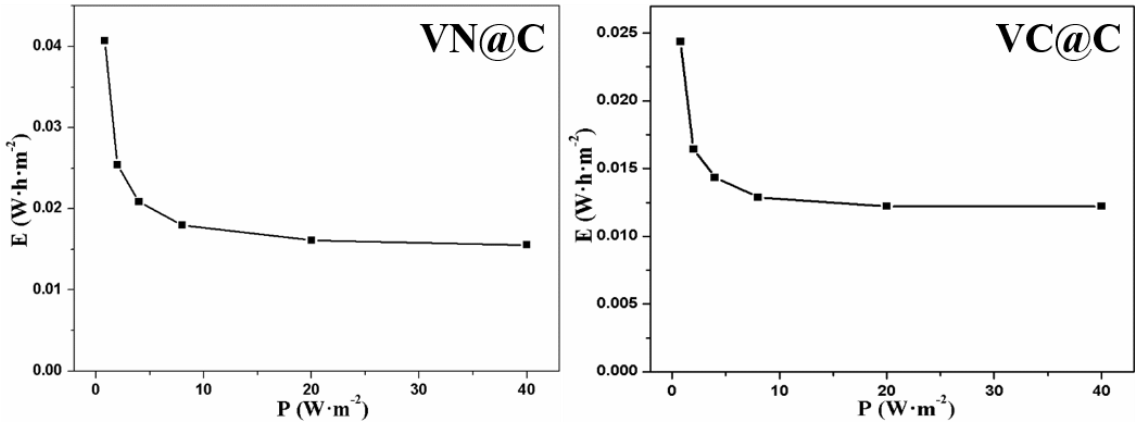

Figure S6. Ragone plots of VN@C SSC device and VC@C SSC device.

Table S1

Table S1. Comparison of the electrochemical performance of various materials based on SC devices.

Various device	Electrolyte	Potential/V	Capacitance /mF·cm^{-2}	Energy density	Power density	Cycling capability	Reference
RGO/Cellulose SSC	H_2SO_4/PVA	0~0.8	46, 2 mV·s^{-1}	15 μWh cm^{-2}	–	99 % after 5000	[4]
Activated carbon cloth SSC	H_2SO_4/PVA	0~1	31, 10 mV·s^{-1}	–	–	95 % after 20000	[5]
Graphene-cellulose tissue composites SSC	H_2SO_4/PVA	0~1.1	80	9 μWh cm^{-2}	100 mW cm^{-2}	90 % after 5000	[6]
Hierarchical carbon tubular nanostructures SSC	H_3PO_4/PVA	0~1	80, 5 mV·s^{-1}	–	–	–	[7]
Hierarchical carbon tubular nanostructures SSC	KOH/PVA	0~1	79, 5 mV·s^{-1}	–	–	–	[7]
Graphite nanosheets/PANI SSC	H_2SO_4/PVA	0~0.8	77.8, 0.1 mA cm^{-2}	–	–	83 % after 10000	[8]
PET/Pt/MnO_2 SSC	H_3PO_4/PVA	0~0.8	20, 10 mV·s^{-2}	1.9*10^{-6} Wh cm^{-2}	1.6*10^{-4} W cm^{-2}	82.2 % after 10000	[9]
V_2O_5 H_2O/graphene SSC	LiCl/PVA	−0.8~0.8	12, 0.25 A·m^{-2}	1.14 μW h cm^{-2}	10.0 μW cm^{-2}	95 % after 2000	[10]
VO_2 NF@3DG SSC	K_2SO_4	−0.6~0.6	70.8, 0.5 mA·cm^{-2}	279.6 mWh m^{-2}	6000 mW m^{-2}	64 % after 3000	[11]
VC@C SSC device	LiCl/PVA	0~0.8	46, 5 mV·s^{-1}	0.024 Wh m^{-2}	0.8 W m^{-2}	81 % after 2000	This work
VN@C SSC device	LiCl/PVA	0~0.8	65, 5 mV·s^{-1}	0.041 Wh m^{-2}	0.8 W m^{-2}	85 % after 2000	This work

ASC = Asymmetric Supercapacitors; SSC = Symmetric Supercapacitors; M = mol L^{-1}; PVA = Polyvinyl Alcohol

References

[1] Y. Zhang, X. Liu, G. Xie, L. Yu, S. Yi, M. Hu, C. Huang, Hydrothermal synthesis, characterization, formation mechanism and electrochemical property of $V_3O_7{\cdot}H_2O$ single-crystal nanobelts, Mater. Sci. Eng. B, 175 (2010) 164-171.

[2] Y. Zhang, X. Liu, D. Chen, L. Yu, J. Nie, S. Yi, H. Li, C. Huang, Fabrication of $V_3O_7{\cdot}H_2O$@C core-shell nanostructured composites and the effect of $V_3O_7{\cdot}H_2O$ and $V_3O_7{\cdot}H_2O$@C on decomposition of ammonium perchlorate, J. Alloys Compd., 509 (2011) L69-L73.

[3] Y. Zhang, M. Zhou, M. Fan, C. Huang, C. Chen, Y. Cao, H. Li, X. Liu, Improvement of the electrochemical properties of $V_3O_7{\cdot}H_2O$ nanobelts for Li battery application through synthesis of V_3O_7@C core-shell nanostructured composites, Curr. Appl. Phys., 11 (2011) 1159-1163.

[4] Z. Weng, Y. Su, D.-W. Wang, F. Li, J. Du, H.-M. Cheng, Graphene–Cellulose Paper Flexible Supercapacitors, Advanced Energy Materials, 1 (2011) 917-922.

[5] G. Wang, H. Wang, X. Lu, Y. Ling, M. Yu, T. Zhai, Y. Tong, Y. Li, Solid-State Supercapacitor Based on Activated Carbon Cloths Exhibits Excellent Rate Capability, Advanced Materials, 26 (2014) 2676-2682.

[6] M. Sevilla, G.A. Ferrero, A.B. Fuertes, Graphene-cellulose tissue composites for high power supercapacitors, Energy Storage Materials, 5 (2016) 33-42.

[7] H. Zhang, H. Su, L. Zhang, B. Zhang, F. Chun, X. Chu, W. He, W. Yang, Flexible supercapacitors with high areal capacitance based on hierarchical carbon tubular nanostructures, Journal of Power Sources, 331 (2016) 332-339.

[8] B. Yao, L. Yuan, X. Xiao, J. Zhang, Y. Qi, J. Zhou, J. Zhou, B. Hu, W. Chen, Paper-based solid-state supercapacitors with pencil-drawing graphite/polyaniline networks hybrid electrodes, Nano Energy, 2 (2013) 1071-1078.

[9] X. Long, Z. Zeng, E. Guo, X. Shi, H. Zhou, X. Wang, Facile fabrication of all-solid-state flexible interdigitated MnO2 supercapacitor via in-situ catalytic solution route, J. Power Sources, 325 (2016) 264-272.

[10] J. Bao, X. Zhang, L. Bai, W. Bai, M. Zhou, J. Xie, M. Guan, J. Zhou, Y. Xie, All-solid-state flexible thin-film supercapacitors with high electrochemical performance based on a two-dimensional $V_2O_5{\cdot}H_2O$/graphene composite, J. Mater. Chem. A, 2 (2014) 10876-10881.

[11] J. Wang, X. Zhang, Y. Zhang, A. Abas, X. Zhao, Z. Yang, Q. Su, W. Lan, E. Xie, Lightweight, interconnected VO2 nanoflowers hydrothermally grown on 3D graphene networks for wide-voltage-window supercapacitors, RSC Adv., 7 (2017) 35558-35564.